

Oblique multi-periscopic prism for field expansion of homonymous hemianopia

MOJTABA FALAHATI,¹ NISH MOHITH KURUKUTI,¹  FERNANDO VARGAS-MARTIN,²  ELI PELI,¹  AND JAE-HYUN JUNG^{1,*} 

¹*Schepens Eye Research Institute of Massachusetts Eye and Ear, Department of Ophthalmology, Harvard Medical School, 20 Staniford St, Boston, MA 02114, USA*

²*Departamento de Electromagnetismo y Electrónica, Universidad de Murcia, Murcia, Spain*
**Jaehyun_Jung@meei.harvard.edu*

Abstract: Oblique Fresnel peripheral prisms have been used for field expansion in homonymous hemianopia mobility such as walking and driving. However, limited field expansion, low image quality, and small eye scanning range limit their effectiveness. We developed a new oblique multi-periscopic prism using a cascade of rotated half-penta prisms, which provides 42° horizontal field expansion along with 18° vertical shift, high image quality, and wider eye scanning range. Feasibility and performance of a prototype using 3D-printed module are demonstrated by raytracing, photographic depiction, and Goldmann perimetry with patients with homonymous hemianopia.

© 2023 Optica Publishing Group under the terms of the [Optica Open Access Publishing Agreement](#)

1. Introduction

Homonymous hemianopia (HH) is a visual impairment represented by blindness of half of the visual field on the same side in both eyes [1]. The visual field loss is caused by brain injuries due to stroke, trauma, tumors, or surgeries [2]. HH causes difficulties in detecting obstacles and avoiding collision with hazards in the blind hemifield, which restricts the patients' mobility and reduces their quality of life. Patient's mobility such as walking in crowded areas, crossing streets, and driving is affected by the HH visual impairment [3–7]. Patients with HH are discouraged from driving due to possible risk of collisions with pedestrians and other cars on their blind side. In most countries of the world and 22 states of the USA, patients with HH are prohibited from driving as they do not meet the minimum required horizontal visual field [8,9].

Eye scanning into the blind side may increase the detection of hazards in the blind hemifield of patients with HH. However, the patients with HH rarely scan more than 15° into the blind side [10–12], and they do not get any clues when to scan. Peli et al. [7] analyzed the risk of collision with other pedestrians while walking in open public spaces such as shopping malls, public plazas, and transportation terminals. Considering all bearing angles for the approaching pedestrians in such unrestricted environments to be equally likely, they found that pedestrians approaching at a 45° bearing angle represent the highest collision risk. The most hazardous bearing angles lie out of the blind field expanded by currently available Fresnel prisms for patients with HH.

High power prisms that deflect rays toward the prism base have been used to shift images of hazards from the blind field of patients with HH into the seeing field. The prisms are mounted on the upper and lower periphery of the seeing hemifield to avoid affecting the central vision (peripheral prisms) [13–15]. Spectacles-mounted peripheral prisms (using Fresnel prism segments) have been used for field expansion of patients with HH [13,16]. Those simple and cost-effective low vision aids are designed to shift image sections of the peripheral field of view laterally from the blind side to the residual seeing side. The original “horizontal” design of the peripheral prisms provided only horizontal field expansion [13], which shows only the upper and lower periphery on the blind side, and thus a central visual gap (the vertical gap between the

upper and lower peripheral prisms) in the blind side was not affected. Unfortunately, this gap coincides with the important view through a typical passenger car windshield [17].

Oblique peripheral prism has been developed to provide vertical shift in addition to lateral shift [18] and thus covers the field of view around the horizontal meridian on the blind side, as the shifted views that help patients with HH in driving [19] and walking [20]. However, the currently available power of Fresnel prism is limited to about 33° , which is not enough to cover the highest risk at 45° bearing angle [7]. With these prisms, the eye scanning toward the blind side is limited by total internal reflection (TIR) to only 5° [21]. The optical quality of these prisms is poor due to spatial distortion, color dispersion, and scatter [22–25].

Recently, a novel horizontal multi-periscopic prism (MPP) using a cascade of half-penta prisms was developed to achieve a wider 45° field expansion with minimal distortion and remarkably better image quality [26]. It also supports up to 15° eye scanning into the blind side. Similar to the horizontal Fresnel peripheral prisms, however, the horizontal MPPs are still incapable of expanding the field of view around the horizontal meridian of the eye [18,20], important for both walking and driving.

Here, we present an oblique MPP that expand the field of view around the horizontal meridian into the blind side as far as the bearing angle (45°) of the highest pedestrian collision risk. Due to the cascading structure of MPP, a multi-axis arrangement of half-penta prisms and cascading configuration are required for the oblique MPP. Obscuration scotomas and spurious reflections should also be considered in the positioning and orientation of the half-penta prism elements. We report optical/mechanical design, development, and validation of our novel oblique MPP for HH mobility (walking and driving). Optical ray tracing and 3D rendering of percept diagram through the oblique MPP are employed to verify designs. We implemented prototypes of the oblique MPPs using 3D-printing technology, which enabled much flexibility in design. The field expansion in the oblique MPP was evaluated using photographic depiction techniques [27] and Goldmann perimetry measured on patients with HH.

2. Method

Half-penta prisms provide deflection based on reflections, reducing refractive optical limitations such as spatial distortion, contrast reduction, and color dispersion. Half-penta prisms consist of one reflecting mirror and one TIR (acting as a mirror) surface intersecting at an angle of 22.5° (Fig. 1(a)), whereby incident rays are deflected by 45° through double reflection (Fig. 1(b)). An $8\text{ mm} \times 8\text{ mm}$ half-penta prism mounted onto a spectacle lens covers about 15° wide field of view through the viewing aperture placed 17 mm in front of the entrance pupil of the eye [27].

As with the oblique Fresnel prism, rotating the half-penta prisms against the incident rays plane (parallel to the horizontal meridian of the eye) results in vertical deflection of the incident rays along with the horizontal deflection as illustrated in Fig. 1(c). The vertical deflection power is $p \cdot \sin(\theta)$, where p is the prism power (in degree) and θ is the prism rotation in degrees, respectively [18]. The horizontal deflection power is reduced by that rotation to $p \cdot \cos(\theta)$. Due to this nonlinear relationship, substantial vertical deflection can be achieved by a slight rotation of the half-penta prism with a much smaller reduction in the horizontal deflection. Due to the peripheral fitting [13,18], the vertical shift is required to show the paracentral view above (below) the horizontal meridian. 20° rotation of half-penta prisms enables 18° of vertical shift while costing only 3° reduction of the lateral shift (to 42°).

Since the half-penta prisms are placed in the upper and lower periphery, their upper and lower translucent (non-imaging) facets cause obscurations, which reduce the vertical field of view (Fig. 2(a)) [26]. Tilting the half-penta prism out (up for the upper segment and down for the lower segment) to match the line of sight eliminates the obscuration scotoma on the half-penta prism closer to the line of sight (Fig. 2(b)). In the far periphery, the obscuration scotomas are

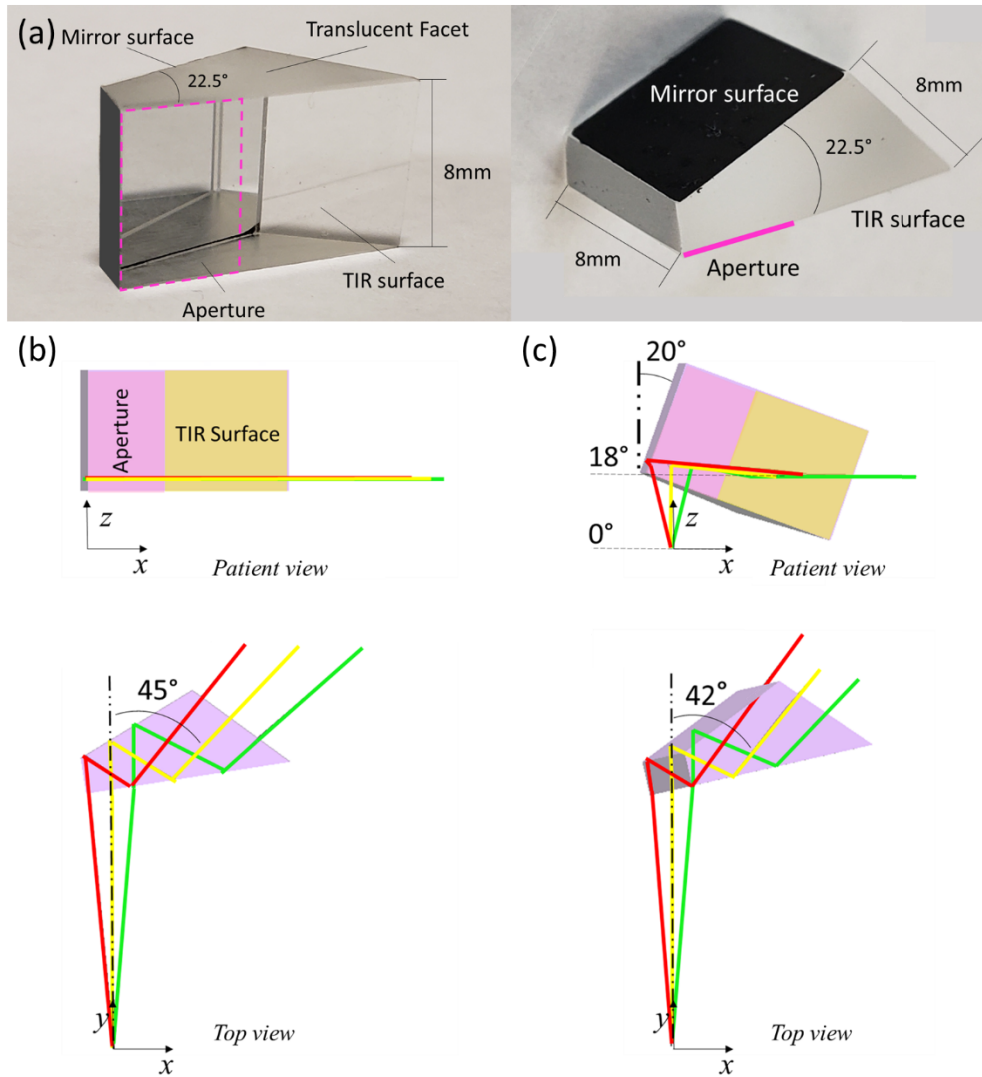


Fig. 1. Half-penta prism rotated to provide both horizontal and vertical deflections. (a) 8×8 half-penta prism. (b) Half-penta prism and (c) rotated half-penta prism by 20° mounted peripherally (18° above the horizontal meridian of the eye) on a spectacles lens (17 mm in front of the entrance pupil of the eye). Double reflection in the half-penta prism provides 45° deflection as shown in the top view of (b), decomposed into 42° horizontal and 18° vertical deflection by the 20° rotation as shown in the top view of (c). (c) The vertical shift in the rotated half-penta prism causes the ray that enters the aperture at 18° vertically from the eye to go to 0° (parallel to the horizontal meridian). There is a small vertical displacement between the deflected rays and the horizontal meridian on the spectacles lens due to the parallel tunnel-field nature [18,26,28–30] which is rapidly diminishing and of negligible effects at the distances of objects of interest.

reduced by these tilts but not eliminated, though these scotomas are inconsequential, as they take place at a very far vertical periphery.

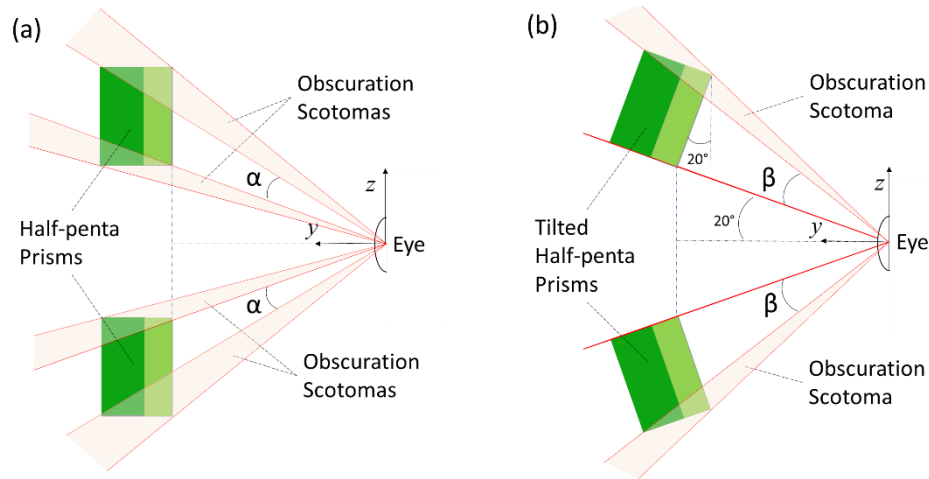


Fig. 2. Tilting half-penta prisms to reduce obscuration scotomas. (a) Upright orientation of the peripheral half-penta prisms shown from the side view. The vertical field of view (α) is limited by the obscuration scotomas at both central and peripheral translucent facets. (b) 20° Tilted peripheral half-penta prisms shown from the side view. The peripheral half-penta prisms are tilted to match the line of sight eliminate and reduce the central and the peripheral obscuration scotomas, respectively, and thus increases the vertical field of view through the device ($\beta > \alpha$).

The horizontal field of view through the peripheral prism needs to equal the horizontal deflection power to allow for a scotoma-free field expansion (with no lateral visual gap between the seeing hemifield and the expanded field toward the blind hemifield) [14,21]. A single oblique half-penta prism (rotated 20°) provides 42° lateral shift but has only 14° horizontal field of view. Thus, cascading a few half-penta prisms is required to create an oblique MPP that matches or exceeds the 42° lateral shift and horizontal field of view.

Figure 3 shows an optical design of the upper oblique MPP cascading five rotated half-penta prisms. The primary half-penta prism (green and intersecting the vertical meridian in Fig. 3) is located on the spectacle carrier lens at 17 mm in front of the entrance pupil and 6 mm above the horizontal meridian ($\sim 20^\circ$), and rotated 20° towards the incident rays (blind side) around the lower corner of the aperture at the opposite side (e.g., for the right HH, the half-penta prism is rotated clockwise around the left lower corner as shown in Fig. 3(c)). The upper primary half-penta prism is also tilted up 20° against the xz -plane to match the line of sight (Fig. 3(d)) and thus avoids the obscuration scotoma by the lower translucent surface. Three similarly rotated and tilted half-penta prisms (purples in Fig. 3(d)) are placed peripherally in a cascade toward the seeing hemifield next to the primary one to cover the 42° horizontal field of view. Each rotated half-penta prism is placed in the cascade with an angle relative to the former one to achieve a multi-faceted aperture that continuously covers the desired field of view, matching the 42° lateral shift. We established the design of the oblique MPP using optical raytracing software (LightTools, Synopsis, Inc., Mountain View, CA). The rotation of the half-penta prisms causes the multi-faceted aperture to be diagonally built up. Each rotated half-penta prism is slightly slid down against the former one to form a horizontal aperture with a zig-zag boundary as shown in Fig. 3(c). The single half-penta prism on the blind side, scanning prism (yellow in Fig. 3), enables field expansion during eye scanning of patient with HH into the blind side up to 14°. Since the incident light is deflected towards the base in conventional prisms, we define the MPP “base”

as the end towards the blind hemifield and “apex” as the opposite end. The Fresnel peripheral prisms are usually mounted on carrier lens on the side of the visual field loss (base-out) [13], but the MPPs are placed on the seeing side lens (base-in, e.g., on the left carrier lens for the right HH) due to longer apex side than base side in MPP. Note the distance from the optical center (pupil position) to the nasal end of the lens in typical spectacles frames is shorter than the temporal end.

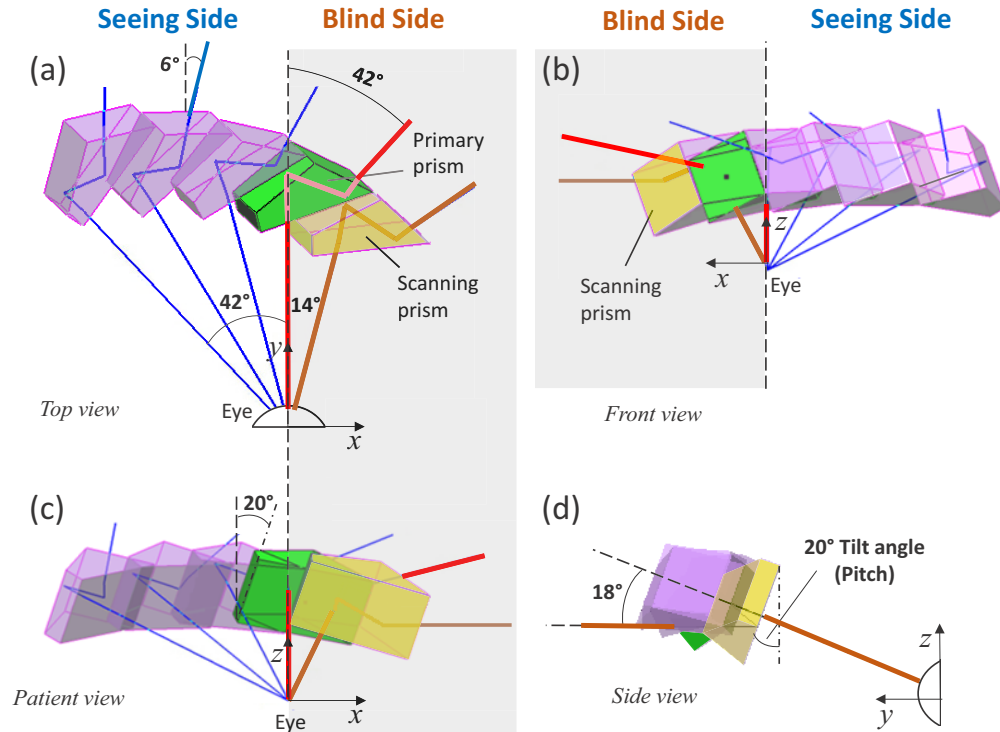


Fig. 3. Optical design of the upper oblique MPP for a right HH cascading five rotated half-penta prisms shown from (a) the top, (b) front, (c) patient, and (d) side views. The primary half-penta prism (green) is rotated by 20° towards the blindside relative to the horizontal plane (c) resulting in 42° lateral (a) and 18° vertical shifts (d) and subsequently 20° tilted up from the horizontal meridian to minimize the obscuration scotoma. The other rotated half-penta prisms (purple) are cascaded into the seeing hemifield to cover the field of view of about 42°. The oblique MPP with five half-penta prisms (shown here) have a slightly wider field of view than the lateral shift magnitude. Thus, the oblique MPP with one less half-penta prisms with a field of view of 14° results in only about 6° apical scotoma (a) between the seeing hemifield and the expanded field into the blind side. The rightmost half-penta prism (yellow) enables eye scanning with field expansion into the blind side up to 14°.

We considered using only four half-penta prisms in the cascade by excluding the farthest one at the seeing side (Fig. 4) to have a lighter and more compact oblique MPP at a lower cost. This provides us with more space at the temporal side to fit the oblique MPP for patients with larger interpupillary distances (IPDs). This results in a small scotoma (~6°) between the expanded field and the residual seeing field (Fig. 3(a)), but small eye scanning (<15°) [11,12] can compensate for this small scotoma.

We simulated the view through the oblique MPP for a user using 3D rendering tool (KeyShot, Luxion Inc. Tustin, CA) (Fig. 4). The pinhole camera is located at the center of the entrance pupil of the eye (17 mm behind the oblique MPP) fixating at the black ball at (0°, 0°). The

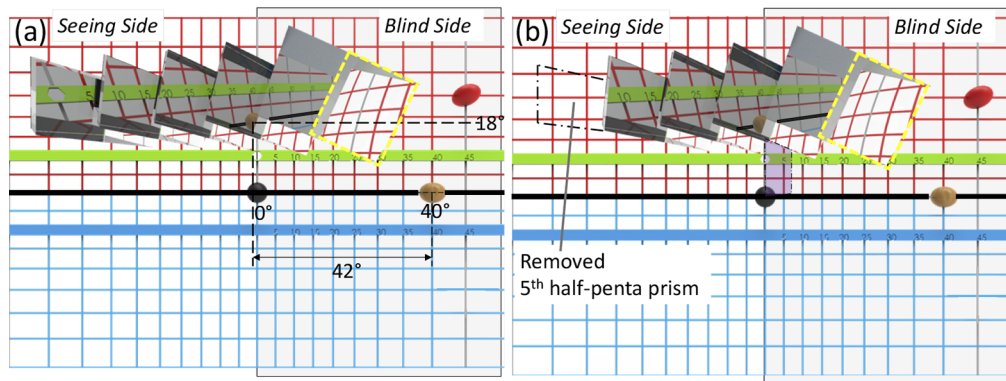


Fig. 4. 3D perspective rendering of percept diagrams through upper oblique MPP based on (a) five half-penta prisms MPP and (b) four half-penta prisms MPP for a patient with right HH. The background is a uniform angular grid with 5° step (i.e., cylindrical projection). A black solid circle is the fixation target (at primary position of gaze). The green bar, 10° above the horizontal meridian, is marked with the angular distances to quantify the lateral image shift through the MPP. The image of the golden ball lying on the horizontal meridian at 40° eccentricity in the blind side can be seen within the primary prism mostly to the left of the vertical meridian demonstrating the 42° horizontal and 18° vertical shift. The hexagon at the center of the green bar is seen in the leftmost (5th) half-penta prism in the oblique MPP in (a). Removing the 5th left most half-penta prism results in about 6° scotoma (field marked by transparent purple) in (b). Note the area marked with the dashed yellow lines on the scanning prism is the TIR surface which needs to be covered by packaging to avoid spurious reflections.

golden ball at 40° lateral eccentricity to the blind side in Fig. 4 can be seen in the primary prism confirming that the oblique MPP enables around 42° lateral and 18° vertical field shifts. Note the multi-faceted aperture of the oblique MPP is partly located about 15° - 32° vertical periphery due to the zig-zag shape though each corner is located at 20° above the horizontal meridian (corresponding vertical field of view from 3° below to 9° above the vertical meridian with 18° vertical shift), which enables showing the object at the horizontal meridian (i.e., the golden ball in Fig. 4). Removing the 5th half-penta prism (the leftmost one) causes a small ($\sim 6^\circ$) paracentral scotoma (Fig. 4(b)). This narrow strip of scotoma can be compensated by slight eye scanning into the blind side.

We developed a 3D printed package to keep complex cascades, rotation, and tilt configurations of the half-penta prisms as an oblique MPP module in position (Fig. 5). We took advantage of the low cost and versatility of the 3D printing technology for prototyping. Due to the required fine features and durability of the holder parts and the required high resolution for precise positioning of the half-penta prisms, we employ the Selective Laser Sintering 3D printing approach which can provide a resolution down to 0.1 mm. The holder parts are made of nylon, which is flexible and sturdy.

The oblique MPP module consists of two interlocking central and peripheral holders for a secure and convenient assembling process. The half-penta prisms fit into corresponding indentations in the peripheral holder. The central holder covers the other side of the cascade and completes the packaging. Minimal thickness was applied in the central holder to reduce the central obscuration while the periphery holder provides the main structural integrity for the whole MPP (Fig. 5). The holders' serrated profile at the lens interface (because of the oblique design) was appropriately trimmed to reduce obscurations to the prism views. Cantilever snap-fit joints were included in the design of the holder components to ease assembly.

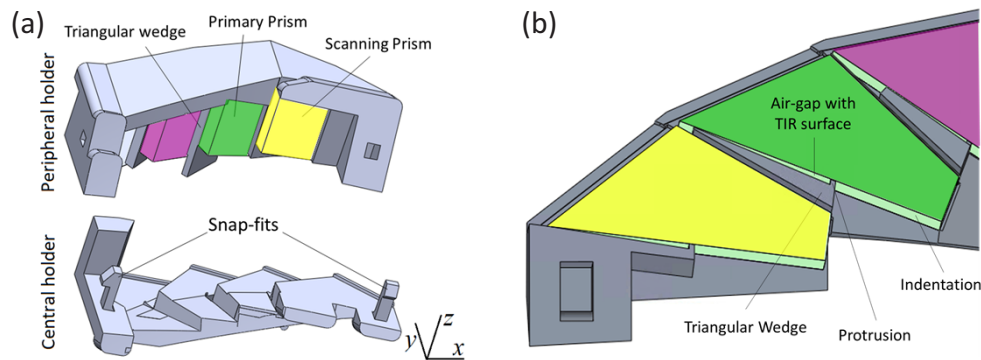


Fig. 5. The upper oblique MPP module. (a) Four half-penta prisms are placed onto the peripheral holder and separated by the triangular wedges. Snap fits at both ends of the central holder allow for glue-free interlocking assembly of the holder parts. (b) The inside view of the peripheral holder; The triangular wedges between each two half-penta prisms in the cascade support the mirror surface of the half-penta prisms on one side. The tiny protrusion on the triangular wedge provides airgap for the TIR surface of the half-penta prism. The translucent upper and lower surfaces are glued onto the indentations in the two holders.

To expand the blind field of view below the horizontal meridian of patients with HH, a lower oblique MPP module is also needed. The lower and upper MPP modules are symmetric with respect to the horizontal meridian except that the scanning prism is removed (Fig. 6) or reduced in size (see discussion) in the lower MPP due to the limited space at the nasal side of the frame caused by the flaring of the nose. Two stubs at the MPPs' module ends fit into corresponding slot cuts into the carrier lens (Fig. 6(a)). The slots in the lens are cut either at the blind side or peripherally far enough above and below the center so that the central area of the carrier lens on

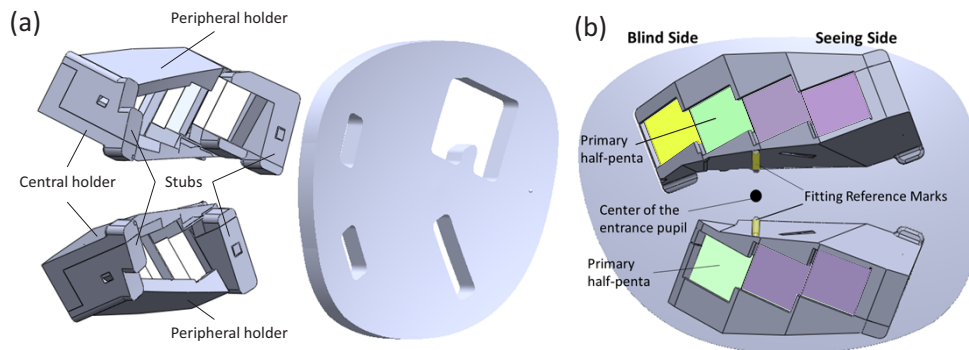


Fig. 6. CAD design of the upper and lower oblique MPP module prototypes for a patient with right HH. (a) Assembled oblique MPP modules enclosed in the peripheral and central holders with stubs, which are ready to fit into the left spectacle lens with corresponding cuttings. The scanning prism in the upper MPP segment partially penetrates the carrier lens. Large opening on the lens corresponding to the stub at the nasal side of the upper oblique MPP prevents lens-prism interference. (b) The oblique MPP fitting reference marks on the central parts of the modules' holders for the right HH can be seen from the front view. The fitting reference marks are provided to verify alignment with the pupil center. Note the pupil center looks off from the primary half-penta in this front view due to the deviated apertures in half-penta prisms.

the seeing side remains intact. Users requiring optical correction benefit from the prescription lens through the oblique MPP.

We added fitting reference marks on the bottom of the upper module and the top of the lower modules to verify and if needed align the pupil of the patient for proper fitting (Fig. 6(b)). Improper lateral alignment may result in discontinuous view across the half-penta prisms, as further discussed in the result section (see Fig. 10).

3. Results

Assembled oblique MPP modules for a patient with right HH mounted on the spectacles left carrier lens in a “base-in” configuration (Fig. 7). The upper and lower MPP optical segments are located about 20° (within 15° - 27° range due to the zig-zag shape of aperture) above and below the horizontal meridian on the carrier lens. The actual inter-prism separation is $\sim 24^\circ$ (i.e., 8 mm on the spectacles lens). A UV-curable optical adhesive is used to fix the oblique MPP stubs into the carrier lens. The oblique MPP system may be realigned with respect to the eyes by adjusting the nose pads so that the pupil markers align with the pupil. The oblique MPPs are mounted unilaterally (i.e., mounted over only one eye) to compensate for the apical scotoma and obscuration scotoma by the fellow eye and thus provide true field expansion under binocular vision [13,14]. The upper and lower oblique MPPs have a dimension of $32\text{ mm} \times 14\text{ mm} \times 13\text{ mm}$ and $31\text{ mm} \times 16\text{ mm} \times 13\text{ mm}$ ($W \times D \times H$), respectively, and weigh 7.6 g and 6.6 g, respectively.

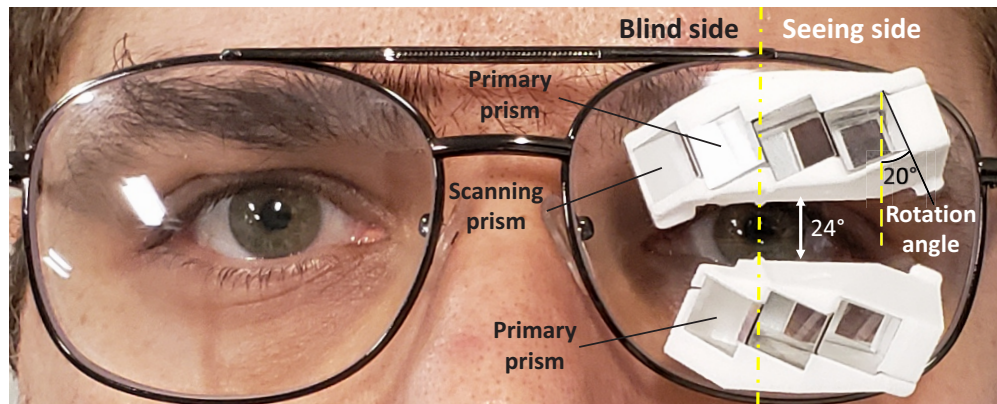


Fig. 7. 3D-printed upper and lower “base-in” oblique MPP prototypes for a patient with right HH. The 3D-printed modules hold the cascade of rotated and tilted half-penta prisms and are mounted on the spectacles. Inter-prism separation allows for vertically 24° wide unobscured central visual field. In this version there is no scanning prism in the lower MPP.

Field expansion with the oblique MPPs on a patient with right HH was measured using binocular Goldmann perimetry (Fig. 8). The upper and lower oblique MPP modules expand the field above and below the horizontal meridian, respectively, in the blind hemifield extended up to 42° . The oblique MPPs provide 18° vertical shifts each and thus a diplopia-free central visual field. Due to the zig-zag shape of the aperture and multiplexing effect (i.e., pupil sharing effect) [26,27], the vertical visual gap between the expanded fields by the upper and lower oblique MPPs was closed.

To illustrate the perceived field and image quality through the oblique MPP in the retinal domain, we used photographic depiction [27]. The oblique MPP modules were mounted 17 mm in front of the entrance pupil of the camera lens to visualize the expected retinal image. We staged a scenario of a potential collision with a pedestrian approaching from the blind side at a bearing angle of about 40° (Fig. 9(a)). Panoramic photograph of the scene (with the subject in the

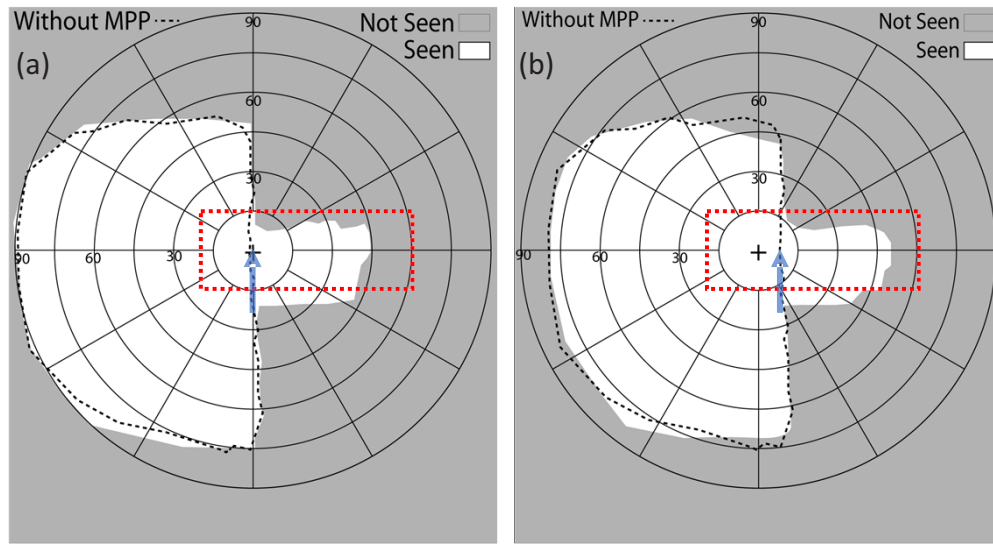


Fig. 8. Binocular Goldmann perimetry of a patient with right HH wearing upper and lower oblique MPPs (a) at the primary position of gaze showing about 43° field expansion into the blind side as well as about 18° vertical shift regardless of eye scanning. The upper and lower expansion join around the horizontal meridian to close the central visual gap (no scotoma), which covers the field of view through a passenger car's windshield (red dotted rectangle). (b) With 10° eye scanning into the blind side (i.e., fixating on the shifted arrow), the oblique MPPs enable an additional 10° lateral field expansion into the blindside. Note the tip of the blue arrow indicates the fixation of the patient. The lower position of the expanded field of view is due to a down head tilt of the patient within the perimeter.

same position) was taken to establish a reference for field shift evaluation. While the pedestrian falls into the blindside (out of the camera's field of view), the upper and lower oblique MPPs shift the pedestrian image onto the seeing field (Fig. 9(b)). The image quality of shifted views through the oblique MPPs is much better than conventional Fresnel prisms [27]. Multiplexing effect [26,27] owing to the camera aperture size ($f/5.6$ matching the indoor photopic pupil size) attenuates the modules' packaging obscuration to a narrow and blurry image boundary.

For a continuous image across the field of view through oblique MPP, the aligned eye pupil position (oblique MPP modules individually fitted for a patient's IPD) is ideal. Lateral offset of the module may result in optical obscuration scotoma between the field of view through the individual half-penta elements in the cascade or may be covered by the multiplexing effect and the tolerance in the cascade design of MPP [26]. To verify, we used the photographic depiction with laterally misaligned oblique MPPs toward the nasal side (fitted for patient with larger IPDs) using two different aperture sizes ($f/22$ and $f/5.6$) at the camera (Fig. 10). While the results with pinhole aperture (the left image in each pair, $f/22$, not possible in human eye) show a sizable obscuration scotoma between the half-penta prisms, the results for the indoor photopic pupil of human eye ($f/5.6$, the right image in each pair,) demonstrate that lateral misalignment of the oblique MPP up to 3 mm causes only lower contrast image with less noticeable obscuration scotoma.

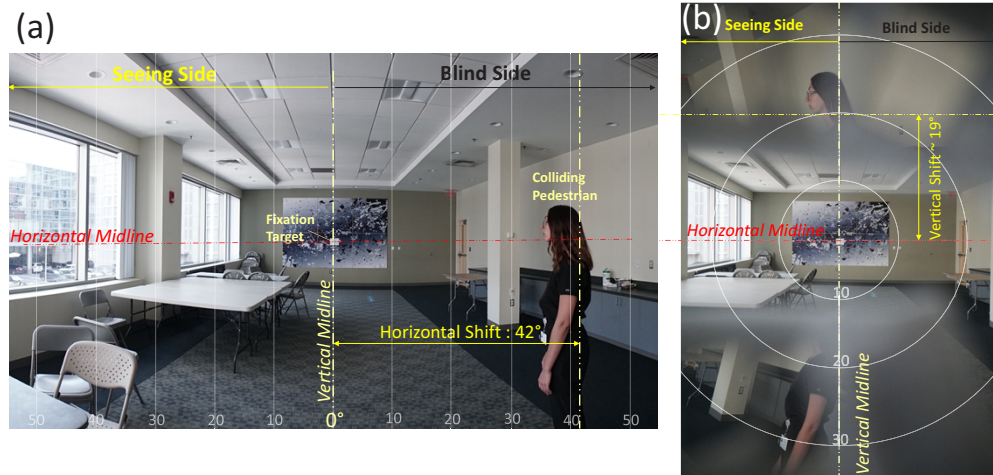


Fig. 9. Photographic depiction through oblique MPPs on the left lens for a patient with right HH. (a) Panoramic picture of the scene showing the angular position of the pedestrian approaching from the blind side at the bearing angle of 40° when the patient is walking toward the fixation target. The chin of the pedestrian is around the horizontal meridian of the patient. At this position, the pedestrian head will not be visible with the horizontal MPP. (b) Photographic depiction of the field of views through the proposed upper and lower oblique MPP segments. The pedestrian's head above the horizontal meridian in the blind field is shifted up about 19° and laterally shifted left by 42° through the upper oblique MPP. The pedestrian's body (below the horizontal meridian) is seen through the lower oblique MPP. Due to the limited camera horizontal field of view, the apex side of the field of view through the oblique MPP is not shown. The obscuration scotomas due to the central holders of the oblique MPPs are seen as narrow low contrast areas (multiplexing effect) above and below the lower and upper prisms views, respectively. Note that the panoramic image (a) is on a cylindrical projection while the photographic depiction of oblique MPP (b) is on perspective projection [27].

4. Conclusion and discussion

The oblique MPP enables a field expansion as wide as 42° around the horizontal meridian in the blind side for mobility assistance which is a substantial improvement in comparison with the current Fresnel oblique prism (only up to 33° with 65 prism diopter). The oblique MPP has many of the advantages of the horizontal MPP such as high prism power, wide eye scanning range, and much better image quality than the Fresnel peripheral prism. Despite the complex cascading and orientation of half-penta prisms in the oblique MPP design, the 3D-printed packaging modules allow for steady mounting, easy assembly, and minimal obscuration. The obscurations, as well as the apical scotomas, are further compensated by the other eye. In addition, the design of the modules is robust over wide range of IPDs (Fig. 10).

One of the most valuable advantages of the oblique MPP is the field expansion available with additional eye scanning into the blindside (up to 14°), which in the Fresnel peripheral prisms was limited by TIR to just 5° [21]. The limited space at the lower part of the spectacles frame deprives the user of the benefit of eye-scanning in the lower oblique MPP. One option is to include a narrower half-penta prism (8×4 mm) as a scanning prism in the lower oblique MPP which can allow for eye scanning up to 7.5° into the blind side (Fig. 11(a)). The smaller size of the half-penta prism also reduce the intrusion of the eye scanning prism into the carrier lens safety margin. Moving the eye scanning prism away from the eye, to avoid intrusion into the carrier lens, may lead to an angular gap between the incident rays striking the primary and eye-scanning prisms,

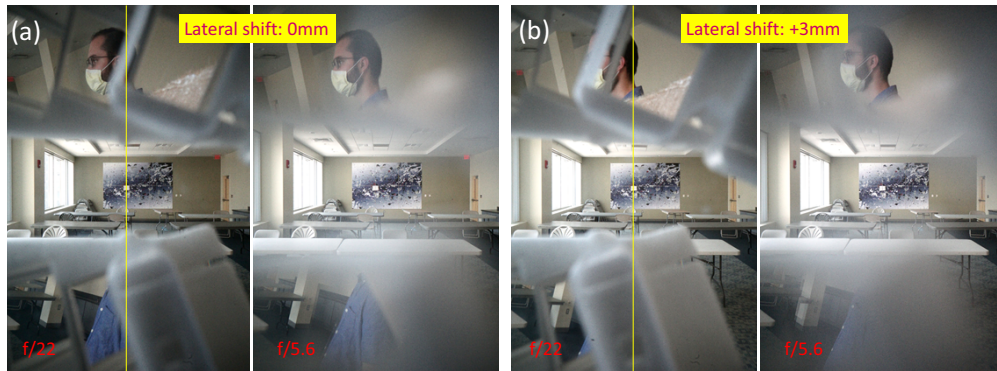


Fig. 10. Photographic depiction of the view through the upper oblique MPP for right HH with lateral misalignment. The potential colliding pedestrian is at 40° eccentricity in the blind side. The oblique MPP is fitted on the carrier lens for 65 mm IPD. The pictures were taken with two different aperture sizes, $f/22$ (pinhole camera) and $f/5.6$ for the indoor photopic pupil of human eye conditions. (a) The actual IPD is 65 mm (no lateral misalignment). The pedestrian head is seen in the primary half-penta prism. The vertical discontinuities between half-penta prisms are visible in the pinhole camera condition ($f/22$) but are not visible in the human eye condition ($f/5.6$). (b) The carrier lens is shifted leftward on the camera lens by 3 mm (representing an IPD of 71 mm). With this shift, the pedestrian head is seen through the scanning half-penta prism and is partially obscured by the package and the scotoma between the two half-penta prisms in the pinhole camera condition. In the human eye condition, however, the vertical obscuration scotoma between the half-penta prisms and the package obscuration turn into lower-contrast areas on the right and thus are less problematic.

which imposes a scotoma between them (Fig. 11(b)). This scotoma, however, may be mitigated by moving the smaller eye-scanning prism slightly to the nasal side. Fortunately, enough room is available for refinement of the packaging mechanical design (Fig. 11c). The benefit of eye scanning may be more important than the remaining scotoma between the two half-penta prisms.

The same 8×4 half-penta prism may be applied to the apex side of the oblique MPP design based on 4 half-penta prisms (Fig. 3) to replace the removed fifth half-penta prism. This will remove the small pericentral scotoma caused by the removal of the fifth Half-penta. The cost/benefit of such modification may need to be considered.

Since the prism provides angular shifts, the perspective viewpoints through and outside of the prism are different [26,27,31]. Such a high-power prism (more rotation) or oblique prism (more tilt) shows more deviations. The oblique MPP that has both higher power and oblique shift results in noticeable rotated and tilted viewpoints (see tilted room column through the oblique MPP in Fig. 9(b)). However, the perspective change of contents may not be an issue for the use of the peripheral prism as collision detection device because the location of the perspective change is in the periphery farther than 20° [26,27,32]. More importantly, this perspective change is reduced when the patient fixates through the oblique MPP (though it is not the correct mode of use of the device).

Since we designed the high prism power to cover around 45° (bearing angle of highest collision risk), we selected and cascaded the half-penta prism as the oblique MPP. Theoretically, half-penta prism-like structure can provide larger than 45° deflection, which may be required to fully cover or cover more than 45° even in the oblique design after the reduction of the lateral shift with the vertical shift [33]. Such additional new developments and refinements of the oblique MPP will be available if any application needs wider field expansion than 45° in oblique configuration.

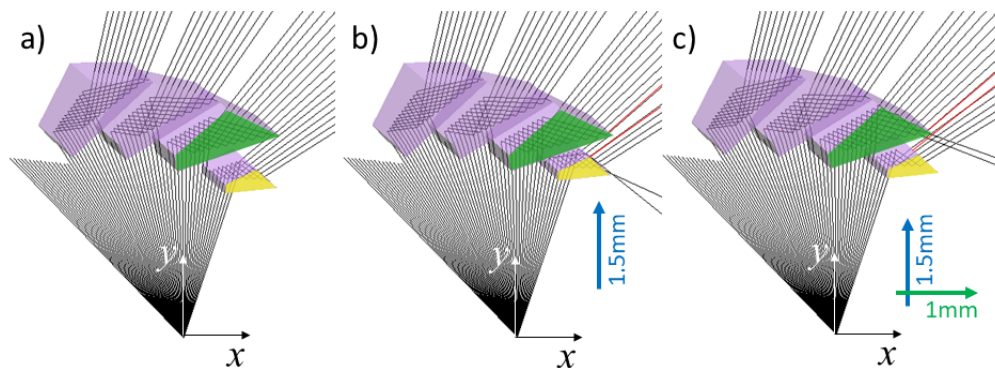


Fig. 11. Using a narrower 8×4 half-penta prism for eye-scanning (yellow) in the lower oblique MPP segment. (a) Positioning of the eye-scanning prism to continuously cover the field of view (i.e., the same position as the 8×8 eye scanning prism in the upper oblique MPP). (b) The eye scanning prism is moved away (1.5 mm forward) from the carrier lens to avoid cutting into the carrier lens. The angular gap between the incident rays (red lines) on the eye-scanning and the primary prism (green) that cause a scotoma between the view through eye-scanning and primary prisms. (c) By additionally moving the eye-scanning prism nasally (1 mm), the angular gap between the incident rays of interest (red lines) decreases.

The MPP prototypes developed in this process are sufficiently efficacious to be used in a clinical trial to determine their effectiveness. We have embarked on such a multi-center clinical trial that will compare the effectiveness of the oblique MPPs against the current oblique Fresnel peripheral prisms (65 prism diopter). If the MPPs prove superior, as we expect, we will have to develop a new design that is aesthetically more attractive or less objectional for patients. It may be worthwhile to determine also if a single (either upper or lower) MPP module will be sufficiently effective, as such design will be much less expensive, lighter in weight, and potentially more attractive. Designing such a reduced size MPP will be an interesting challenge.

Funding. National Eye Institute (P30EY003790, R01EY23385).

Disclosures. Drs. Peli and Vargas-Martin have a patent for the MPP assigned to the Schepens Eye Research Institute and the Universidad de Murcia, Spain.

Data availability. No data were generated or analyzed in the presented research.

References

1. X. Zhang, S. Kedar, M. J. Lynn, N. J. Newman, and V. Biousse, "Natural history of homonymous hemianopia," *Neurology* **66**(6), 901–905 (2006).
2. B. B. Bruce, X. Zhang, S. Kedar, N. J. Newman, and V. Biousse, "Traumatic homonymous hemianopia," *Journal of Neurology, Neurosurgery, and Psychiatry* **77**(8), 986–988 (2006).
3. S. A. Haymes, A. W. Johnston, and A. D. Heyes, "Relationship between vision impairment and ability to perform activities of daily living," *Ophthalmic Physiol. Opt.* **22**(2), 79–91 (2002).
4. E. Papageorgiou, G. Hardiess, F. Schaeffel, H. Wiethoelter, H. O. Karnath, H. Mallot, B. Schoenfish, and U. Schiefer, "Assessment of Vision-Related Quality of Life in Patients with Homonymous Visual Field Defects," *Graefes Arch. Clin. Exp. Ophthalmol.* **245**(12), 1749–1758 (2007).
5. C. S. Chen, A. W. Lee, G. Clarke, A. Hayes, S. George, R. Vincent, A. Thompson, L. Centrella, K. Johnson, A. Daly, and M. Crotty, "Vision-related quality of life in patients with complete homonymous hemianopia post stroke," *Top. Stroke Rehabil.* **16**(6), 445–453 (2009).
6. A. R. Bowers, "Driving with homonymous visual field loss: a review of the literature," *Clin. Exp. Optom.* **99**(5), 402–418 (2016).
7. E. Peli, H. Apfelbaum, E. L. Berson, and R. B. Goldstein, "The risk of pedestrian collisions with peripheral visual field loss," *J. Vis.* **16**(15), 5 (2016).
8. C. F. Alberti, E. Peli, and A. R. Bowers, "Driving with hemianopia: III. Detection of stationary and approaching pedestrians in a simulator," *Invest. Ophthalmol. Vis. Sci.* **55**(1), 368–374 (2014).

9. E. Peli and D. Peli, *Driving with Confidence: A Practical Guide to Driving with Low Vision* (World Scientific Publishing, 2002), p. 192.
10. R. R. Gameiro, K. Junemann, A. Herbig, A. Wolff, P. König, and M. B. Hoffmann, "Natural visual behavior in individuals with peripheral visual-field loss," *J. Vis.* **18**(12), 10 (2018).
11. F. Vargas-Martin and E. Peli, "Eye movement patterns in walking hemianopic patients (abstract)," *Invest. Ophthalmol. Vis. Sci.* **43**, S3809 (2002).
12. G. Luo, F. Vargas-Martin, and E. Peli, "The role of peripheral vision in saccade planning: Learning from people with tunnel vision," *J. Vis.* **8**(14), 25 (2008).
13. E. Peli, "Field expansion for homonymous hemianopia by optically-induced peripheral exotropia," *Optom. Vis. Sci.* **77**(9), 453–464 (2000).
14. H. L. Apfelbaum, N. C. Ross, A. R. Bowers, and E. Peli, "Considering apical scotomas, confusion, and diplopia when prescribing prisms for homonymous hemianopia," *Transl. Vis. Sci. Technol.* **2**(4), 2 (2013).
15. J.-H. Jung and E. Peli, "No useful field expansion with full-field prisms," *Optom. Vis. Sci.* **95**(9), 805–813 (2018).
16. A. R. Bowers, K. Keeney, and E. Peli, "Randomized crossover clinical trial of real and sham peripheral prism glasses for hemianopia," *JAMA Ophthalmol.* **132**(2), 214–222 (2014).
17. F. Vargas-Martin and M. A. Garcia-Perez, "Visual fields at the wheel," *Optom. Vis. Sci.* **82**(8), 675–681 (2005).
18. E. Peli, A. R. Bowers, K. Keeney, and J. H. Jung, "High-power prismatic devices for oblique peripheral prisms," *Optom. Vis. Sci.* **93**(5), 521–533 (2016).
19. K. E. Houston, E. Peli, R. B. Goldstein, and A. R. Bowers, "Driving with hemianopia VI: Peripheral prisms and perceptual-motor training improve blind-side detection in a driving simulator," *Transl. Vis. Sci. Technol.* **7**(1), 5 (2018).
20. N. M. Kurukuti, K. Tang, J.-H. Jung, and E. Peli, "Effect of peripheral prism configurations on pedestrian collision detection while walking (Abstract)," *Invest. Ophthalmol. Vis. Sci.* **61**, 2771 (2020).
21. J.-H. Jung and E. Peli, "Impact of high power and angle of incidence on prism corrections for visual field loss," *Opt. Eng.* **53**(6), 061707 (2014).
22. K. Ogle, "Distortion of the Image by Ophthalmic Prisms," *AMA Archives of Ophthalmology* **47**(2), 121–131 (1952).
23. K. Ogle, "Distortion of the image by prisms," *J. Opt. Soc. Am.* **41**(12), 1023–1028 (1951).
24. M. Katz, "Contrast sensitivity through hybrid diffractive, Fresnel, and refractive prisms," *Optometry* **75**(8), 509–516 (2004).
25. D. Cheng and G. C. Woo, "The effect of conventional CR39 and Fresnel prisms on high and low contrast acuity," *Ophthalmic Physiological Opt.* **21**(4), 312–316 (2001).
26. E. Peli, F. Vargas-Martin, N. M. Kurukuti, and J.-H. Jung, "Multi-periscopic prism device for field expansion," *Biomed. Opt. Express* **11**, 4872–4889 (2020).
27. J.-H. Jung, N. M. Kurukuti, and E. Peli, "Photographic Depiction of the Field of View with Spectacles-mounted Low Vision Aids," *Optom Vis Sci.* **98**, 1210–1226 (2021).
28. B. B. Bruce and N. J. Newman, "Functional visual loss," *Neurol. Clin.* **28**(3), 789–802 (2010).
29. P. Satgunam, H. L. Apfelbaum, and E. Peli, "Volume perimetry: measurement in depth of visual field loss," *Optom. Vis. Sci.* **89**(9), E1265–E1275 (2012).
30. J.-H. Jung and E. Peli, "Field expansion for acquired monocular vision using a multiplexing prism," *Optom. Vis. Sci.* **95**(9), 814–828 (2018).
31. J.-H. Jung and E. Peli, "Apparent viewpoint of shifted view through prisms," *Invest. Ophthalmol. Visual Sci.* **62**, 1445 (2021).
32. C. Qiu, J.-H. Jung, M. Tuccar-Burak, L. P. Spano, R. B. Goldstein, and E. Peli, "Measuring the effects of prisms on pedestrian collision detection with peripheral field loss," *Transl. Vis. Sci. Technol.* **7**(5), 1 (2018).
33. H. J. Choi, E. Peli, M. Park, and J.-H. Jung, "Design of 45° periscopic visual field expansion device for peripheral field loss," *Opt. Commun.* **454**, 124364 (2020).